

PETROLOGICAL ANALYSIS OF THE THYLACINE SANDSTONE MEMBER

SORELL BASIN

Monique Warrington
Santos Ltd

1. INTRODUCTION

Santos Ltd. has a strong exploration acreage position in the Sorell Basin, a southern oblique-slip extension of the Otway Basin, is located offshore south eastern Australia (Figure 1). Late Cretaceous reservoir sandstones, belonging to the Waarre Formation, Flaxman Formation and Thylacine Sandstone Member, form the main productive zones within the fields, such as Casino, Minerva, La Bella, Thylacine and Geographe. These sandstones typically exhibit excellent reservoir quality with average log porosity in the range of 15-28% and permeabilities of up to 8 Darcies. Reservoirs are typically extensive and homogeneous.

The Thylacine Sandstone Member exhibits some variability in reservoir quality associated with diagenesis. Thirteen samples were selected from key wells, Geographe-1, Thylacine-2, Whelk-1 and Prawn-A1 (Table 1), for detailed petrological description of thin sections and scanning electron microscopy (SEM). The aims of the study were to ascertain the lithology, mineralogy, sediment provenance, diagenetic alteration and factors controlling reservoir quality within these four wells.

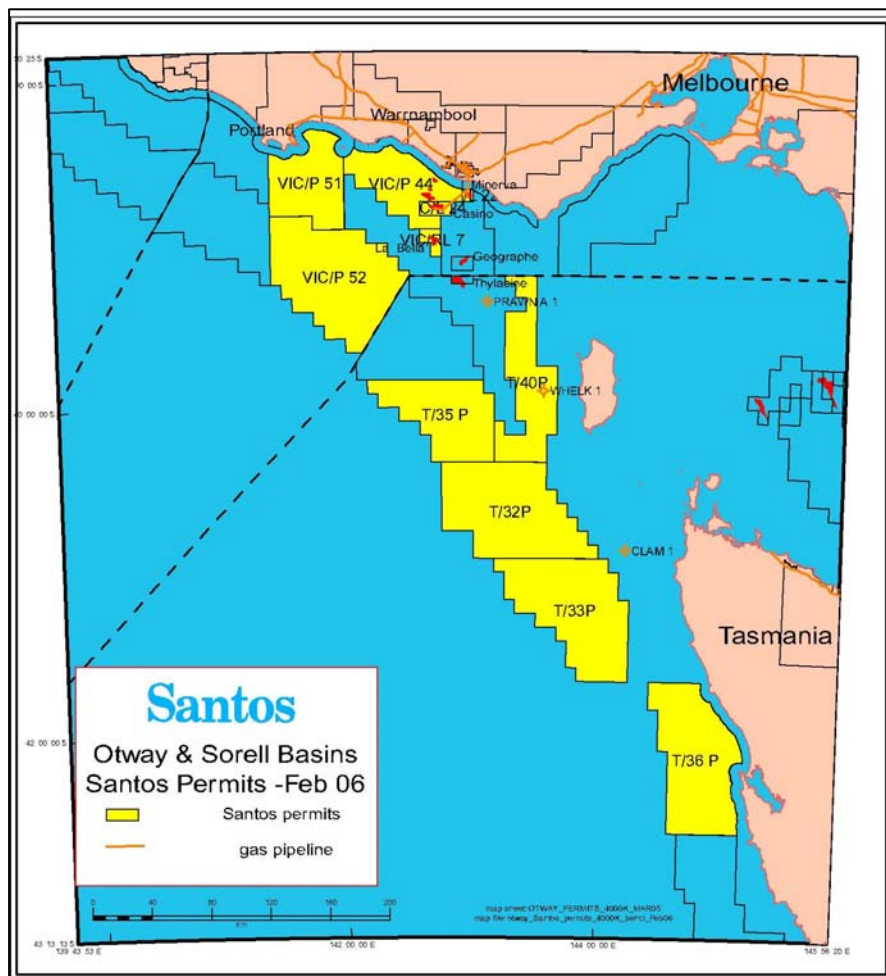


Figure 1: Location map

Sample	Depth (m)	TS Description	Grain size analysis	Point count	SEM
<i>Geographe-1</i>					
	1836.8	✓	✓	✓	
	1839.5	✓	✓	✓	
	1907.5	✓	✓	✓	✓
	1908.2	✓	✓	✓	✓
	1908.9	✓	✓	✓	✓
	1909.8	✓	✓	✓	✓
<i>Thylacine-2</i>					
	2175.5	✓	✓	✓	
	2185.55	✓	✓	✓	
	2228.82	✓	✓	✓	
	2229.62	✓	✓	✓	
<i>Prawn-A1</i>					
	2030.73	✓	✓	✓	
	2032.25	✓	✓	✓	
<i>Whelk-1</i>					
	1293.88	✓	✓	✓	

Table 1: Samples analysed

2. METHODOLOGY

Thin section

Sidewall cores were prepared by Pontifex and Associates, Adelaide. Blue-stained araldite was impregnated into each sample to aid with the discrimination of porosity and voids of plucked grains. Petrographic analysis of thin sections was undertaken using an Olympus BHSP microscope with an Olympus 2500L camera attached. Representative photomicrographs showing features of interest were taken under both plane and cross polarized light.

Petrographic data attained from thin sections included depositional and diagenetic fabrics, mineralogic compositions, fabric analysis and the determination of the sequence of diagenetic events. Siliciclastics have been classified according to guidelines by Folk (1974) and carbonates are classified using the nomenclature of Tucker (2001). Grain morphology (both sphericity and roundness) was estimated from diagrams after Harrell, J. (1984) and sorting from diagrams in Boggs (2001). Percentages of composition given in the thin section descriptions are attained from counts of 400 points.

Scanning electron microscopy (SEM)

Scanning electron microscope analysis was undertaken on broken segments of samples mounted with araldite on aluminum stubs and coated with gold/platinum at Adelaide Microscopy. The 4 samples were analysed using a Phillips XL20 scanning electron microscope.

NOTE: Examples of typical petrographic features are illustrated in Figures 2.10-2.13

3. PETROLOGY

TABLE 2. POINT COUNT DATA

WELL	Geographe-1	Geographe-1	Geographe-1	Geographe-1	Geographe-1
Stratigraphic Unit	Upper TSM	Upper TSM	Lower TSM	Lower TSM	Lower TSM
Depth (mRT)	1836.8	1839.5	1907.5	1908.2	1908.9
Lithology	Sublitharenite	Sublitharenite	Sublitharenite	Sublitharenite	Sublitharenite
Avg GS (mm)	0.15	0.2	0.18	0.16	0.16
Sorting	Moderate	Poor	Moderate	Moderate	Poor
Roundness	A-SR	A-R	A-SR	SSE-SR	A
Sphericity	SE-SS	SE-SS	E-SS	SE-SS	E-SS
	<i>Volume Percentage</i>				
Framework grains					
Quartz					
- Mono	27.33	28.00	25.66	26.33	31
- Poly	8.33	5.66	12.66	12.66	8.66
Feldspar	0.33	0.66	2.66	1.66	1.33
Lithics			7.33	6.0	7.33
- sedimentary	5.33	4.66			
- metamorphic	1.33	0.0			
- igneous	1.00	0.33			
Mica	0.33	0.33	0.66	0.33	0.66
Accessory	2.00	0.33	2.33	0.66	0.66
Other	Tr	0.33	1.33	1.33	0.0
Matrix	1.66	0.0	1.33	0.33	1.33
Authigenic minerals					
Glaucony	Tr	Tr	0.0	0.0	0.0
Quartz	4.00	2.33	Tr	Tr	Tr
Feldspar	0.0	0.0	Tr	Tr	Tr
Kaolin					
- replace	6.00	2.66	9.06	9.0	13.33
- pore fill	11.33	0.33	5.66	4.0	2.66
Illite – replace	0.66	0.33	0.66	0.33	1.66
Carbonate					
- replace	11.66	53.00	15.0	18.33	18.33
- pore fill	8.00	0.0	0.33	0.0	0.0
Porosity					
Intergranular	1.33	0.0	0.33	1.0	3.33
Dissolution	5.33	0.66	11.0	13.0	5.66
Micropores	4.00	0.66	4.0	5.0	5.0
Fracture	0.0	0.0	0.0	0.0	0.0

TABLE 3. POINT COUNT DATA

WELL	Geographe-1	Thylacine-2	Thylacine-2	Thylacine-2	Thylacine-2
Stratigraphic Unit	Lower TSM	Lower TSM	Lower TSM	Lower TSM	Lower TSM
Depth (mRT)	1909.8	2175.5	2185.55	2228.82	2229.62
Lithology	Sublitharenite	Sublitharenite	Sublitharenite	Sublitharenite	Sublitharenite
Avg GS (mm)	0.16	0.2, 0.4	0.12, 0.25	0.3	0.25
Sorting	Poor	Poor	Poor	Moderate	Poor
Roundness	SA-SR	SA-R	A-SR	SA-SR	SA-SR
Sphericity	E-SS	SE-S	E-SS	E-SS	E-SS
	<i>Volume Percentage</i>				
<i>Framework grains</i>					
Quartz					
- Mono	24.66	36.66	29.33	39.00	30.00
- Poly	10.33	9.66	10.00	9.33	4.33
Feldspar	0.66	Tr	0.33	0.0	Tr
Lithics	3.0				
- sedimentary		9.66	7.00	6.33	3.66
- metamorphic		3.00	3.66	3.0	1.0
- igneous		2.00	2.00	0.66	0.66
Mica	1.0	0.33	1.33	1.66	0.33
Accessory	0.33	1.00	0.66	0.33	0.0
Other	1.0	0.0	0.0	0.0	0.0
<i>Matrix</i>	0.0	4.0	9.66	8.66	4.00
<i>Authigenic minerals</i>					
Glaucony	0.0	Tr	Tr	0.0	Tr
Quartz	Tr	6.0	3.66	8.0	4.00
Feldspar	Tr	0.0	0.0	0.0	0.0
Kaolin					
- replace	0.0	0.89	1.11	1.77	1.55
- pore fill	2.66	12.67	10.67	10.00	4.44
Illite – replace	0.0	0.33	0.0	0.0	0.0
Carbonate					
- replace	55.06	0.0	9.00	0.33	41.66
- pore fill		2.66	3.66	1.33	0.33
<i>Porosity</i>					
Intergranular	0.0	1.0	0.33	0.33	0.0
Dissolution	0.0	3.33	1.66	3.00	1.00
Micropores	1.33	6.77	5.88	5.89	3.00
Fracture	0.0	0.0	0.0	0.0	0.0

TABLE 4. POINT COUNT DATA

WELL	Whelk-1	Prawn-A1	Prawn-A1
Stratigraphic Unit	TSM	TSM	TSM
Depth (mRT)	1293.88	2030.73	2032.25
Lithology	Sublitharenite	Sublitharenite	Sublitharenite
Avg GS (mm)	0.25	0.3, 0.8	0.2
Sorting	Well	Poor	Moderate
Roundness	A-SR	SA-R	A-SR
Sphericity	E-S	E-S	E-SS
	<i>Volume Percentage</i>		
<i>Framework grains</i>			
Quartz			
- Mono	31.66	42.66	41.00
- Poly	10.66	12.00	5.33
Feldspar	0.66	Tr	1.33
Lithics			
- sedimentary	7.66	5.0	6.0
- metamorphic	5.33	4.33	3.0
- igneous	5.00	3.0	2.33
Mica	2.00	Tr	2.0
Accessory	0.33	0.33	0.0
Other	Tr	0.0	0.0
<i>Matrix</i>	2.66	4.33	3.33
<i>Authigenic minerals</i>			
Glaucony	Tr	Tr	Tr
Quartz	4.66	5.33	8.66
Feldspar	0.0	0.0	0.0
Kaolin			
- replace	0.66	0.44	0.22
- pore fill	2.89	1.67	4.0
Illite – replace	0.0	0.0	0.0
Carbonate			
- replace	0.3	3.33	4.0
- pore fill	0.66	1.33	1.66
<i>Porosity</i>			
Intergranular	6.33	4.0	4.33
Dissolution	16.66	7.66	10.66
Micropores	1.77	3.55	2.11
Fracture	0.0	0.0	0.0

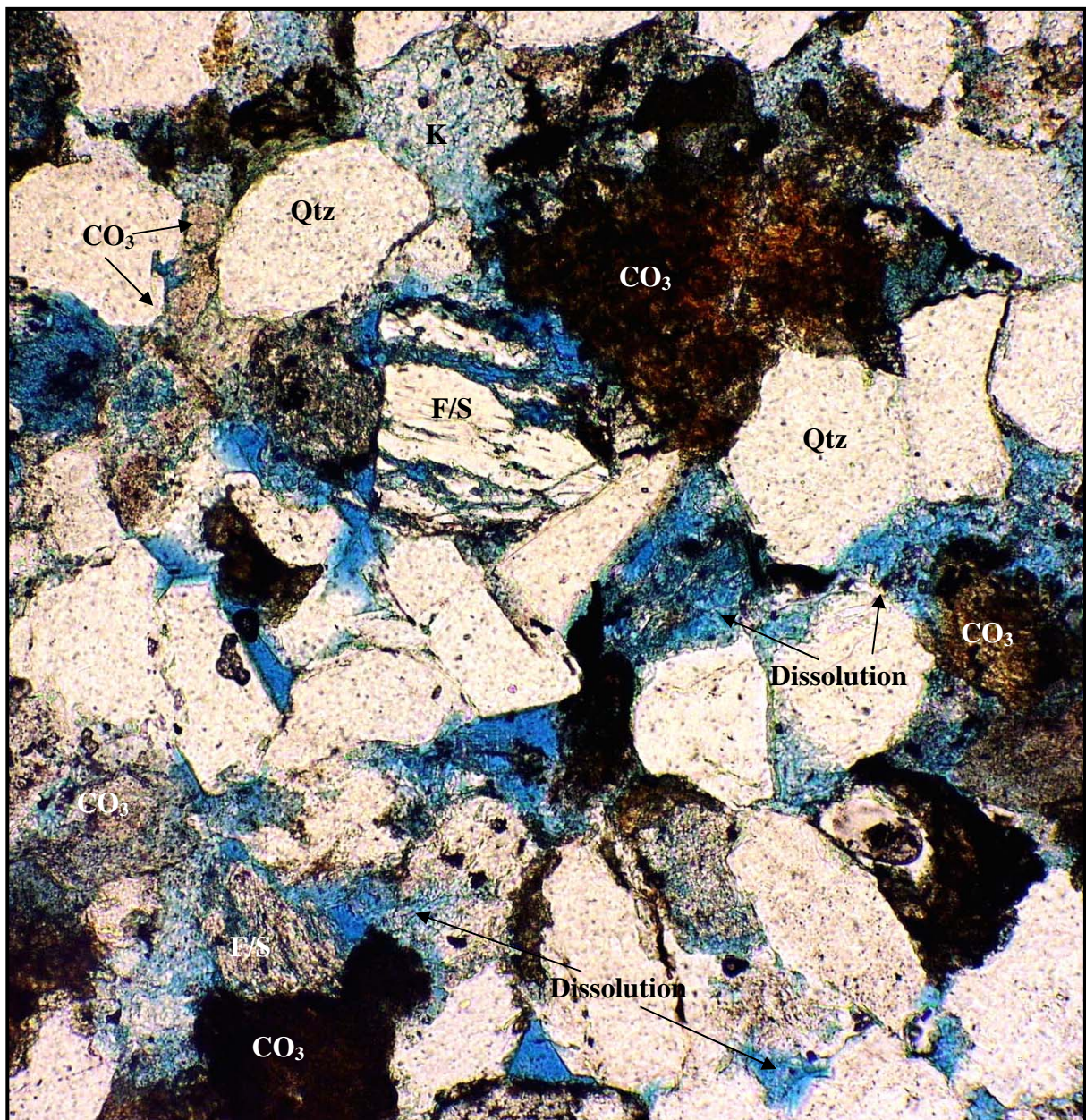


Figure 2.1

General field of view. Large secondary pores which are commonly partly filled with both loosely-packed and tightly-packed kaolin. Siderite occurs as micrite and spar, filling pore spaces and replacing grains. All feldspar grains are either partially dissolved, primarily along cleavage traces or replaced. Estimated porosity in this field of view is 15%. Connectivity between the open pores is generally via masses of loosely packed kaolin. Geographe-1, 1836.8m, plane light, 10 microns

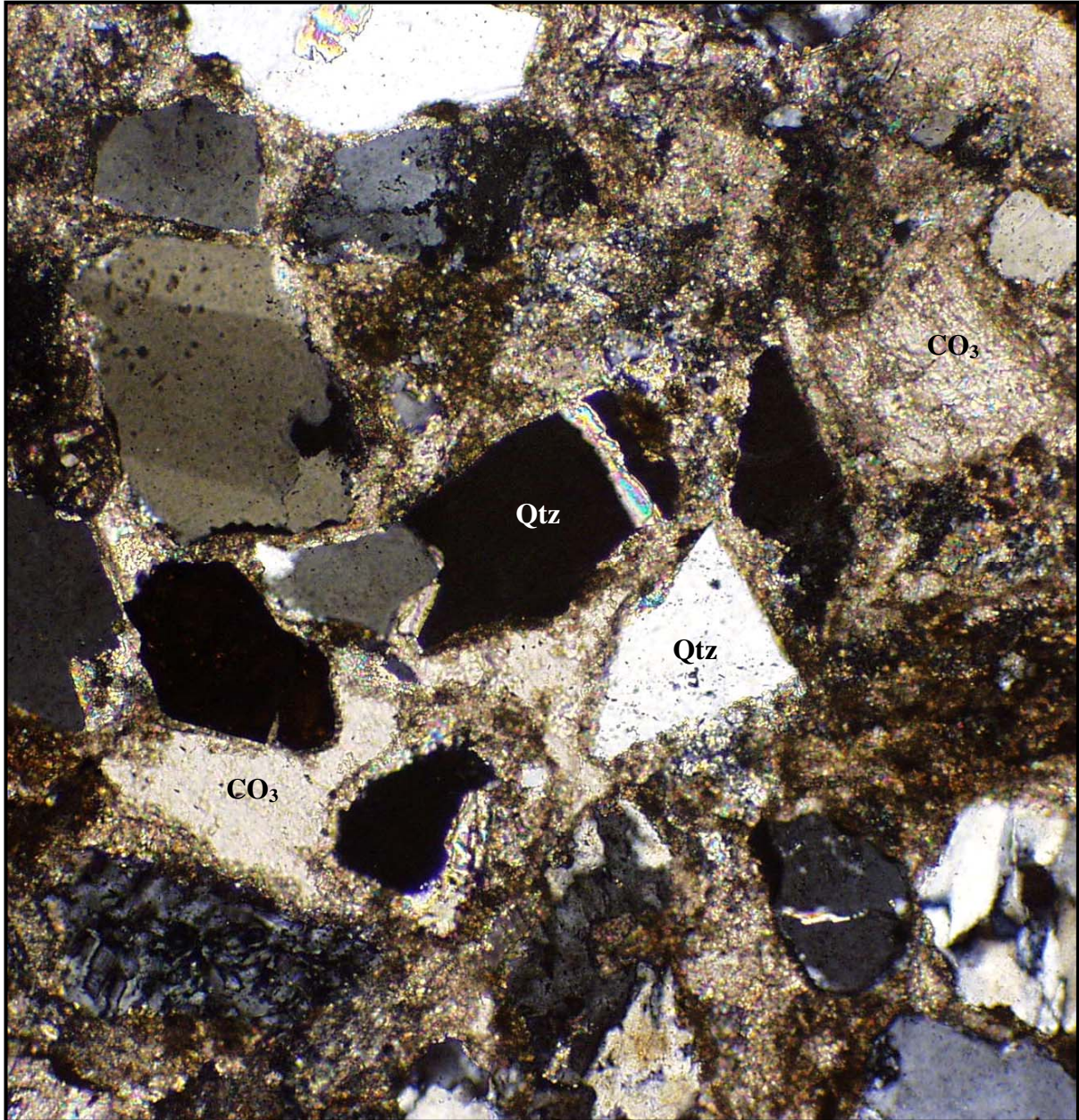


Figure 2.2

Pervasive carbonate cement fills pore spaces and partially replaces framework grains. Both metamorphic and igneous quartz are observed. There is no visible porosity in this field of view although some could exist within the kaolin masses.

Geographe-1, 1839.5m, cross-polarised light, 10 microns.

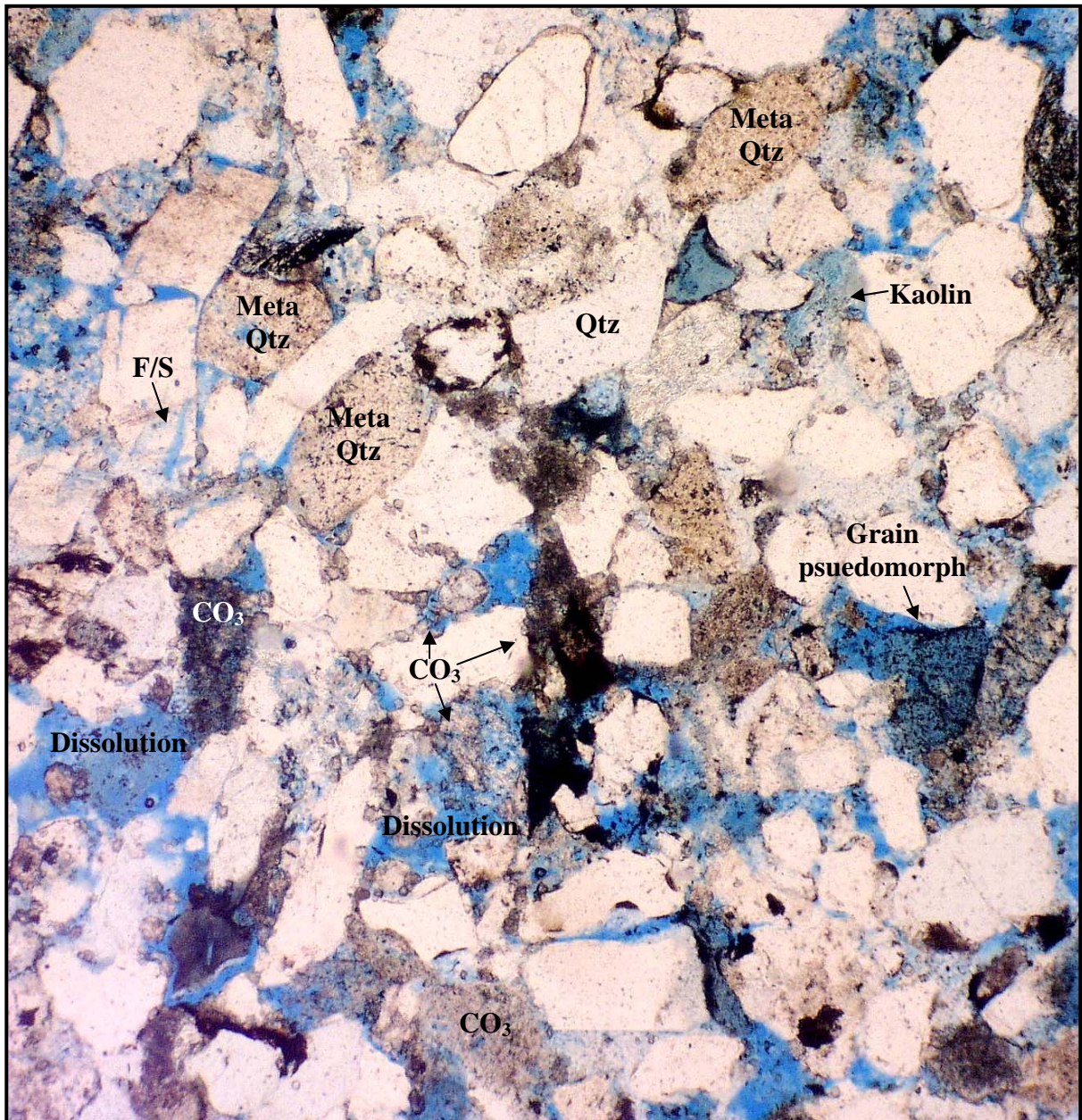


Figure 2.3

Typical field of view illustrating the dominance of secondary and micro pores within this sublitharenite. Feldspar dissolution adds to the patchy primary porosity but both pore types are modified by loosely-packed kaolin. The 15% point count porosity in this sample is largely secondary (11%) and micro (1%).

Geographe-1, 1907.5m, plane light, 5 microns.

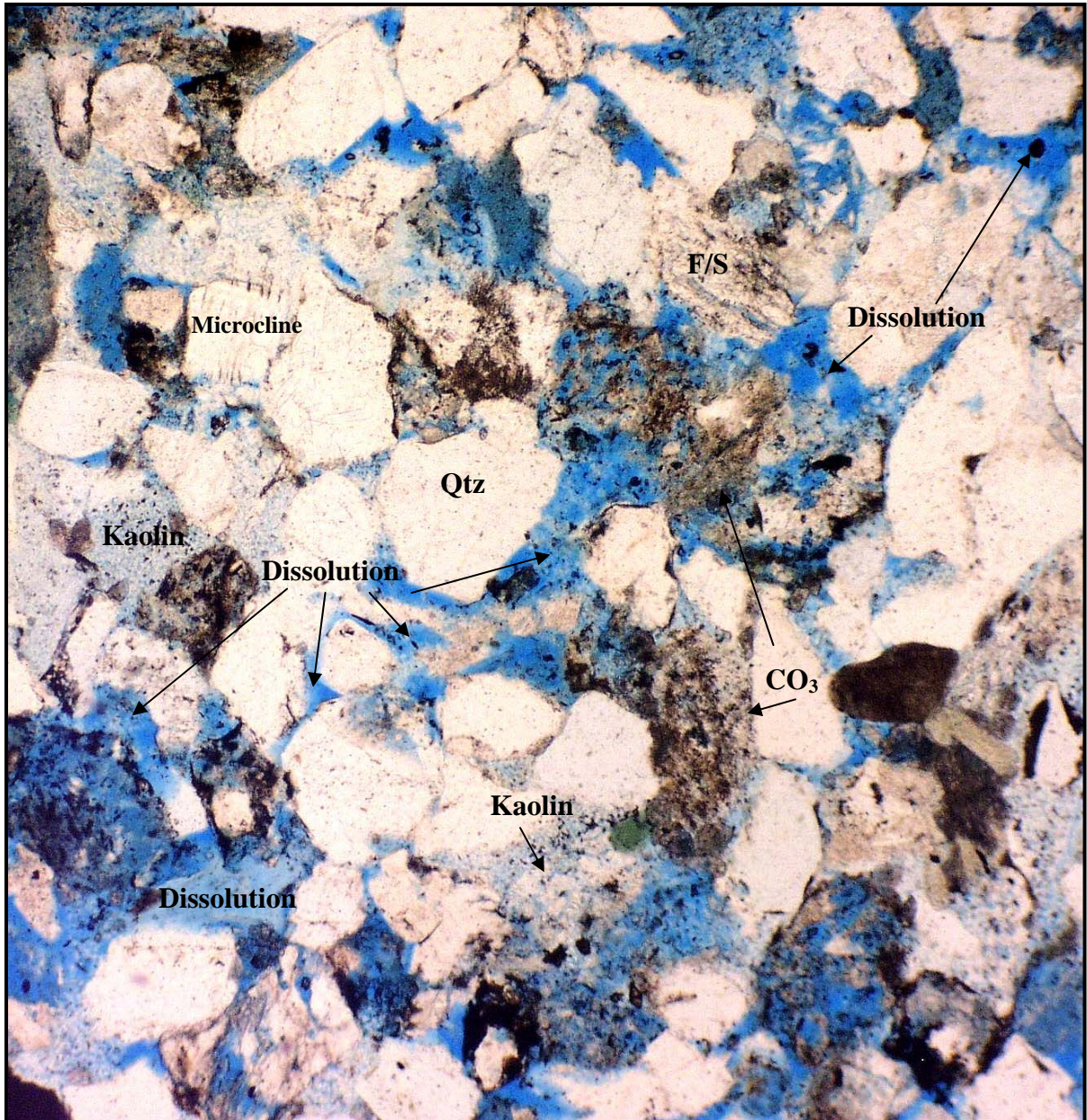


Figure 2.4

General field of view illustrating the dominance of grain-sized dissolution pores and areas of loosely-packed kaolin (speckled) with associated micropores. The quartz grains are mainly igneous and volcanic types. The carbonate content is high and rock fragments moderate. Point counting suggested 13% secondary porosity and 5% microporosity.

Geographe-1, 1908.2m, plane light, 5 microns.

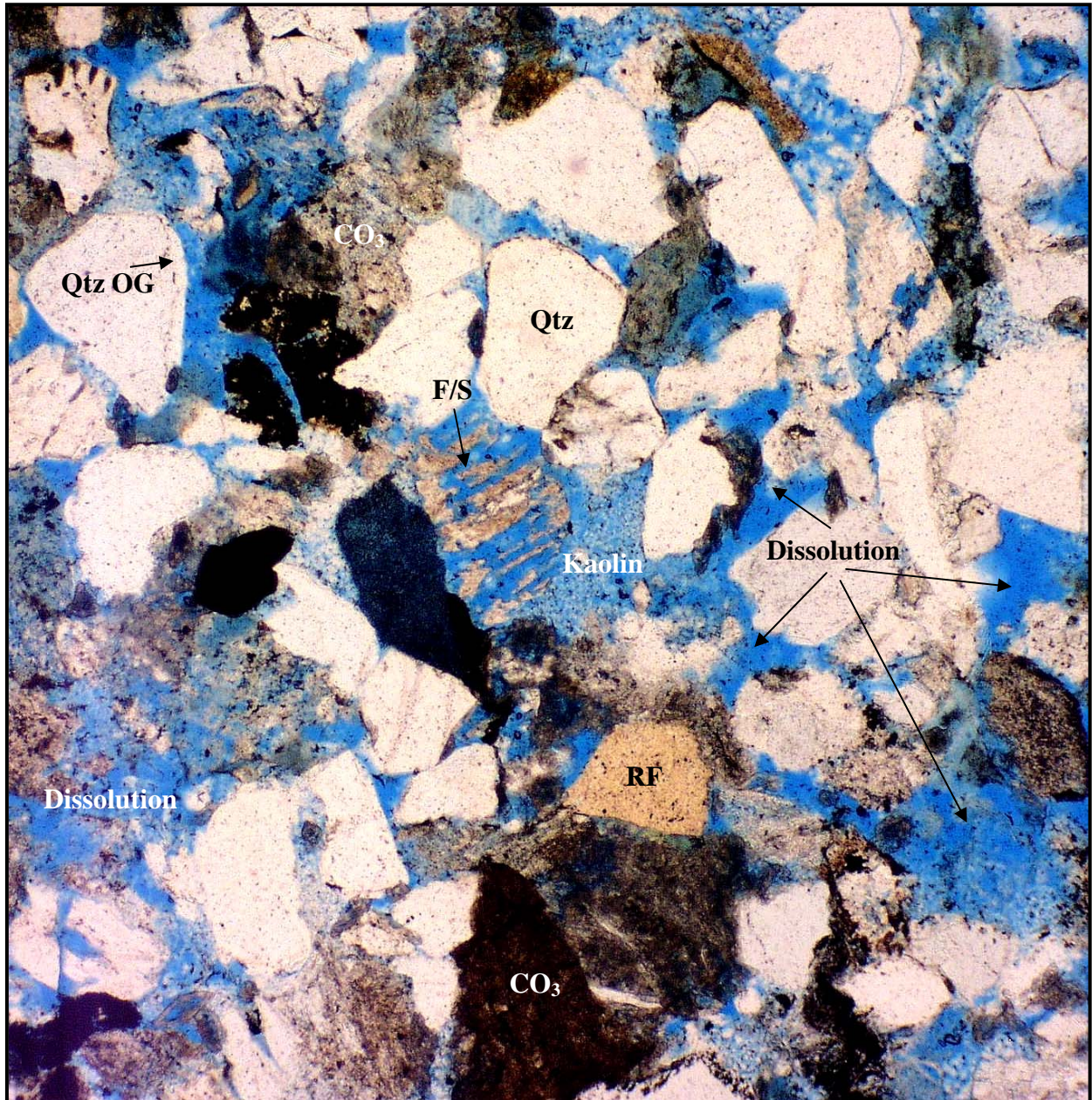


Figure 2.5

A moderately sorted, sublitharenite illustrating reasonable porosity and good connectivity between pores. Grains are dominantly angular and largely consist of quartz, rock fragments with replacement kaolin and carbonate. Dissolution and micropores constitute the main pore types, 5.7% and 5% respectively. The secondary pores add to the existing primary porosity, suggesting good permeability.
 Geographe-1, 1908.9m, plane light, 5 microns.

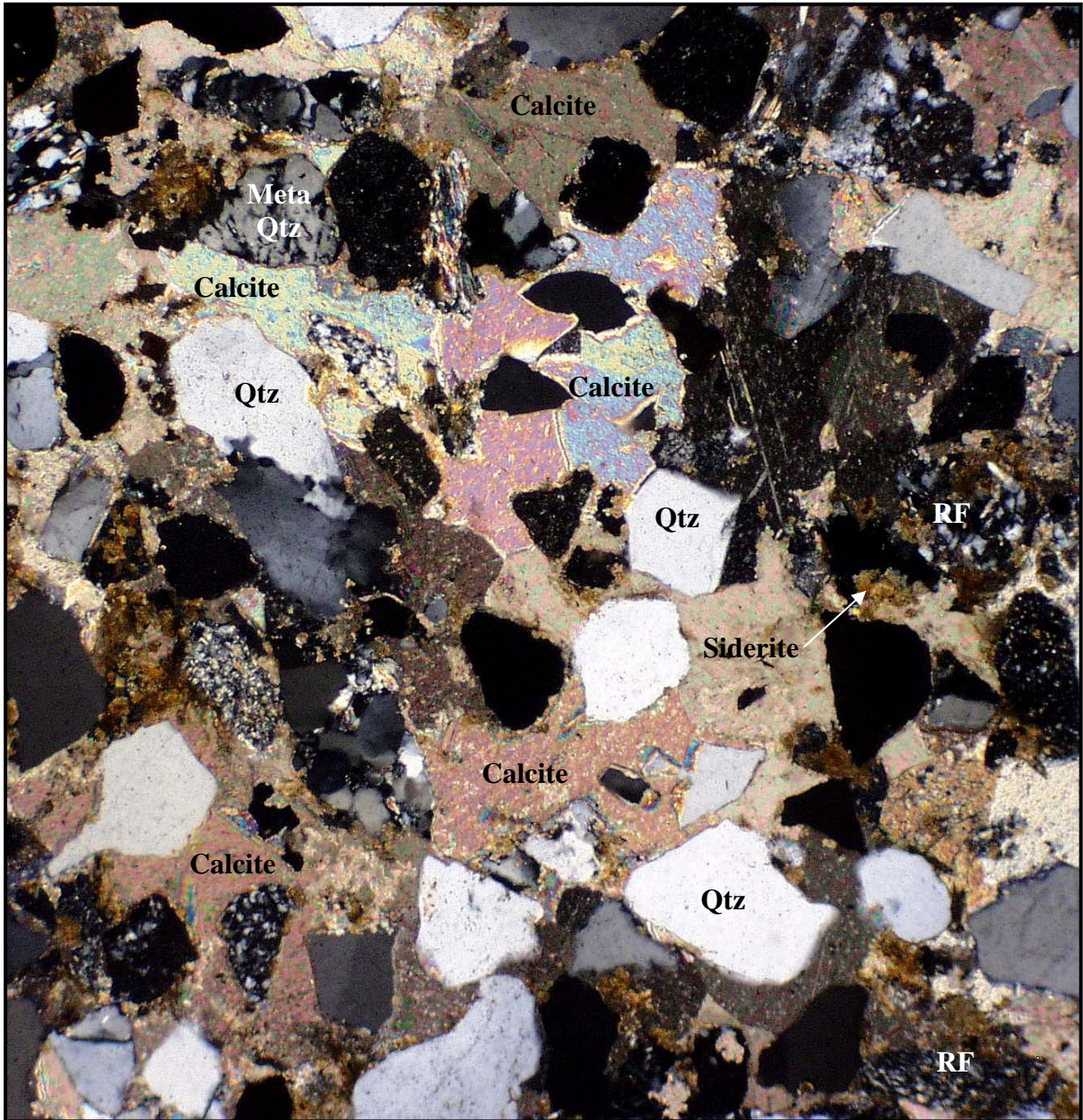


Figure 2.6

Typical field of view illustrating the packing and highly altered nature of the framework grains. Replacement calcite is pervasive to the extent that the residual framework grains are floating in the carbonate cement. Very limited remnants of intergranular pores are apparent and these may be secondary in nature.

Geographe-1, 1909.8m, cross-polarized light, 5 microns.

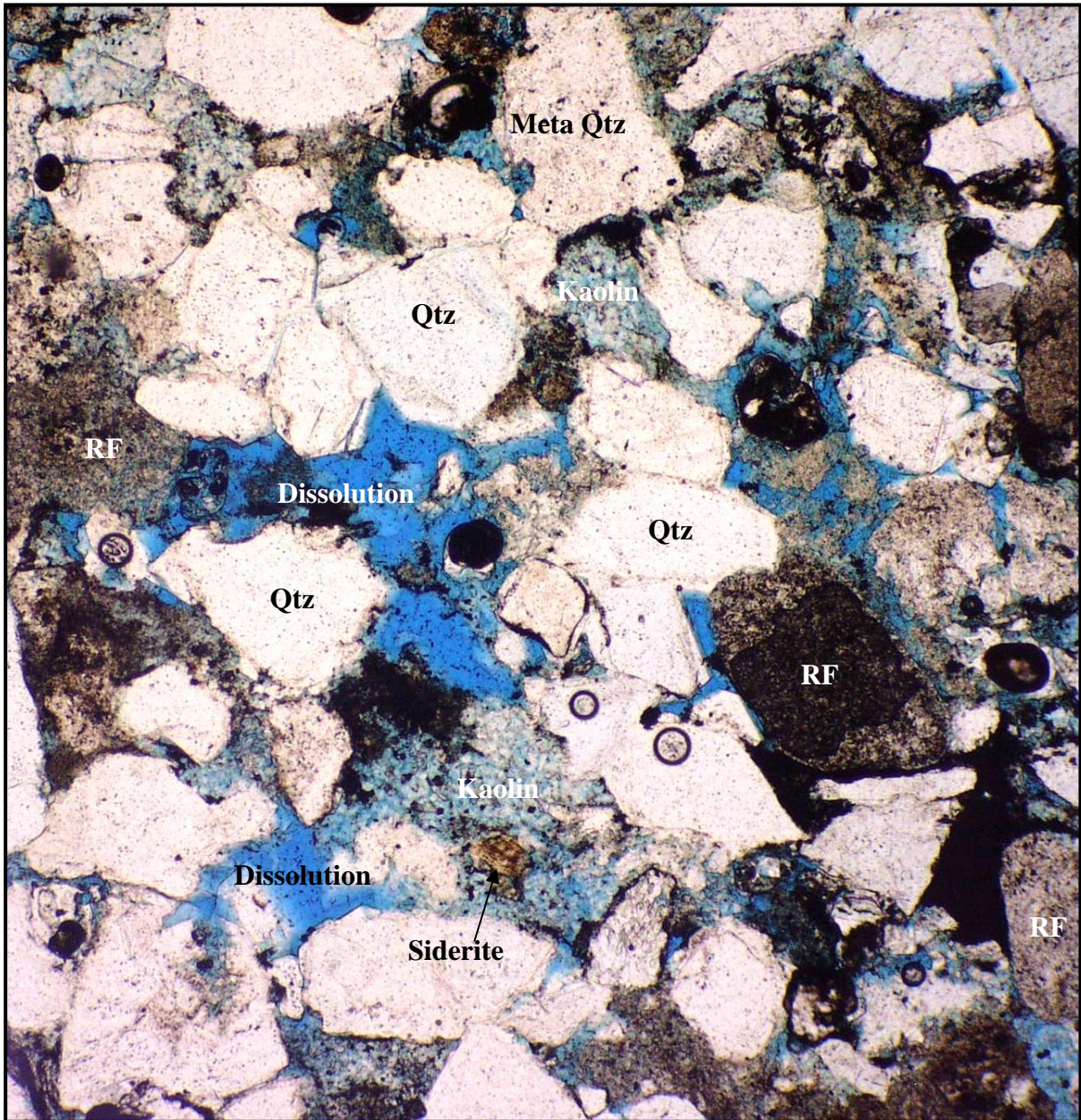


Figure 2.7

Poorly sorted sandstone containing a high amounts of volcanic quartz, pore-filling kaolin and rock fragments. Sedimentary rock fragments include chert, while metamorphic rock fragments are typically mica-bearing but quartz-rich. Pores have reasonable connectivity and are rarely filled with carbonate.

Thylacine-2, 2175.5m, plane light, 5 microns.

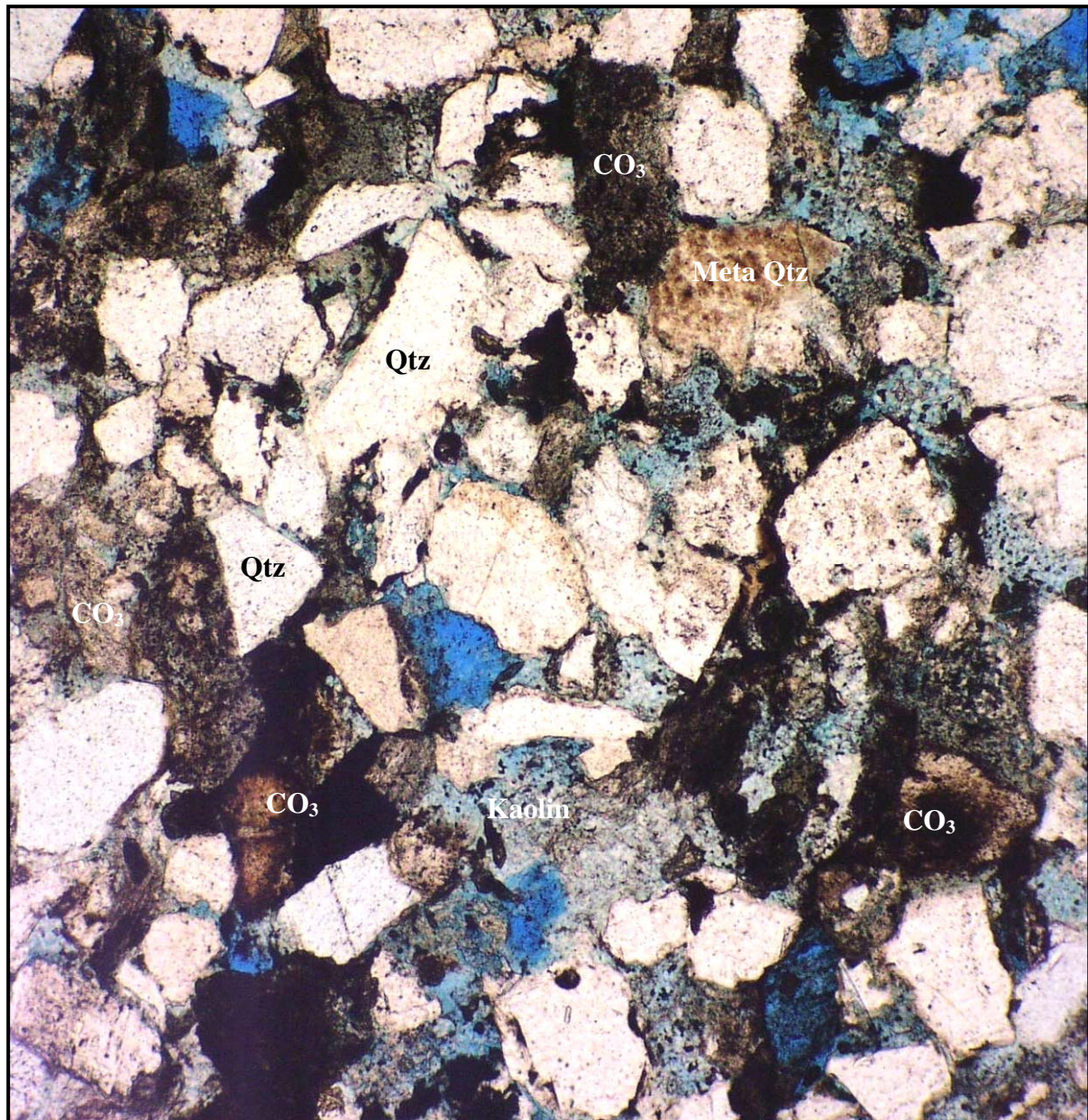


Figure 2.8

Poorly sorted sandstone with a bimodal grain-size distribution. Matrix, kaolin and/or carbonate fill most pore spaces, with the remainder being poorly interconnected. Late carbonate is observed as replacing grains in heavily cemented bands. Kaolin replaces feldspars and rock fragments and, as such, is densely packed. Pores are not well connected, suggesting low permeability. Thylacine-2, 2185.55m, plane light, 5 microns

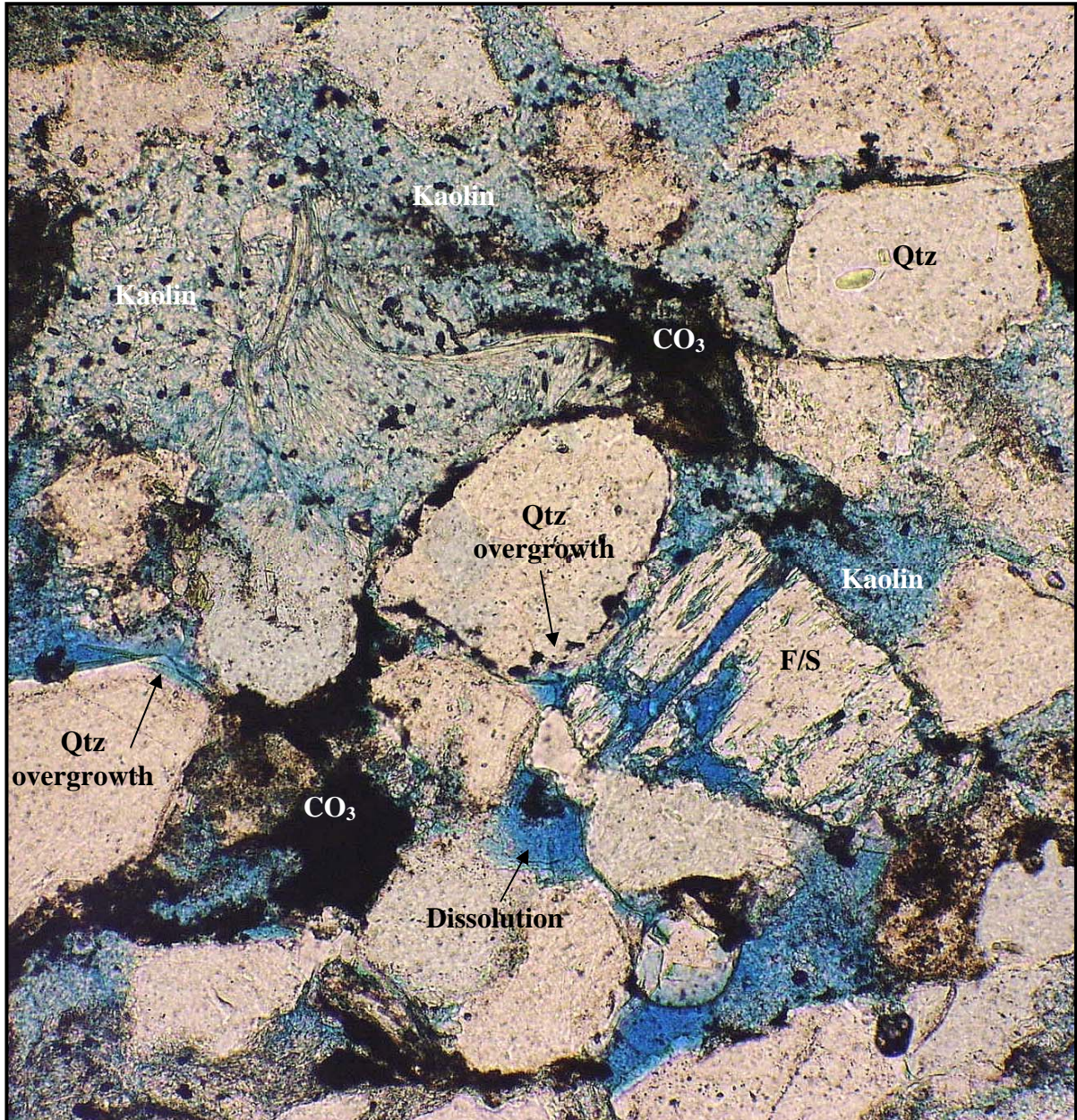


Figure 2.9

General field of view illustrating a large quantity of pore-filling kaolin and an increase in quartz overgrowths. Well rounded grains are typically observed beneath the overgrowths. Carbonate (siderite and dolomite) content is significantly reduced. Feldspar grains illustrate preferential dissolution along cleavage traces. Connectivity between the 3% secondary pores is via the masses of kaolin with their associated microporosity, suggesting the sample overall has low permeability.

Thylacine-2, 2228.82m, plane light, 10 microns.

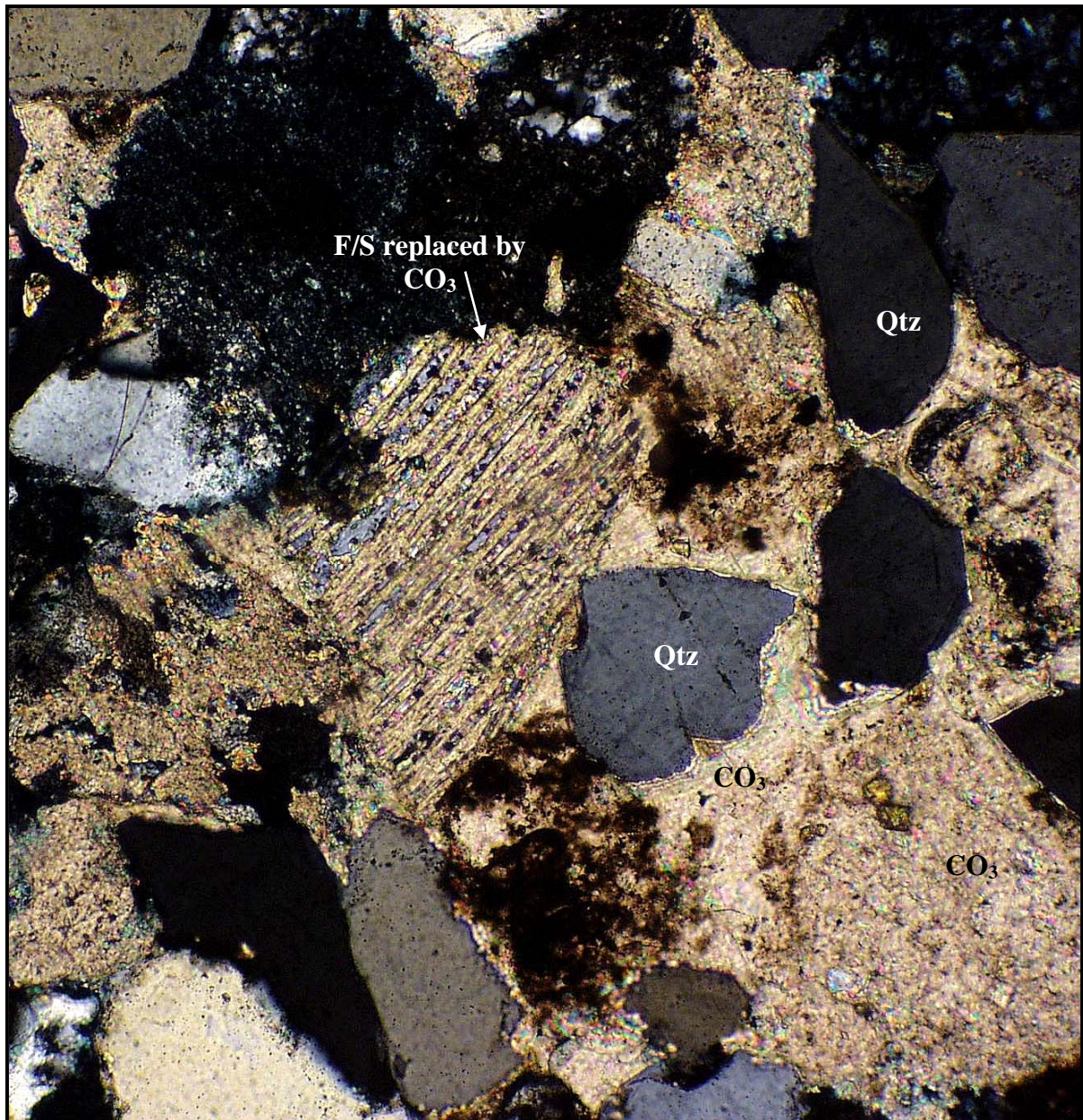


Figure 2.10

This sublitharenite consists largely of pervasive calcite and siderite cement which has replaced most grains. No primary porosity was observed however the carbonate has not eradicated all micro-porosity.

Thylacine-2, 2229.62m, cross-polarised light, 10 microns.

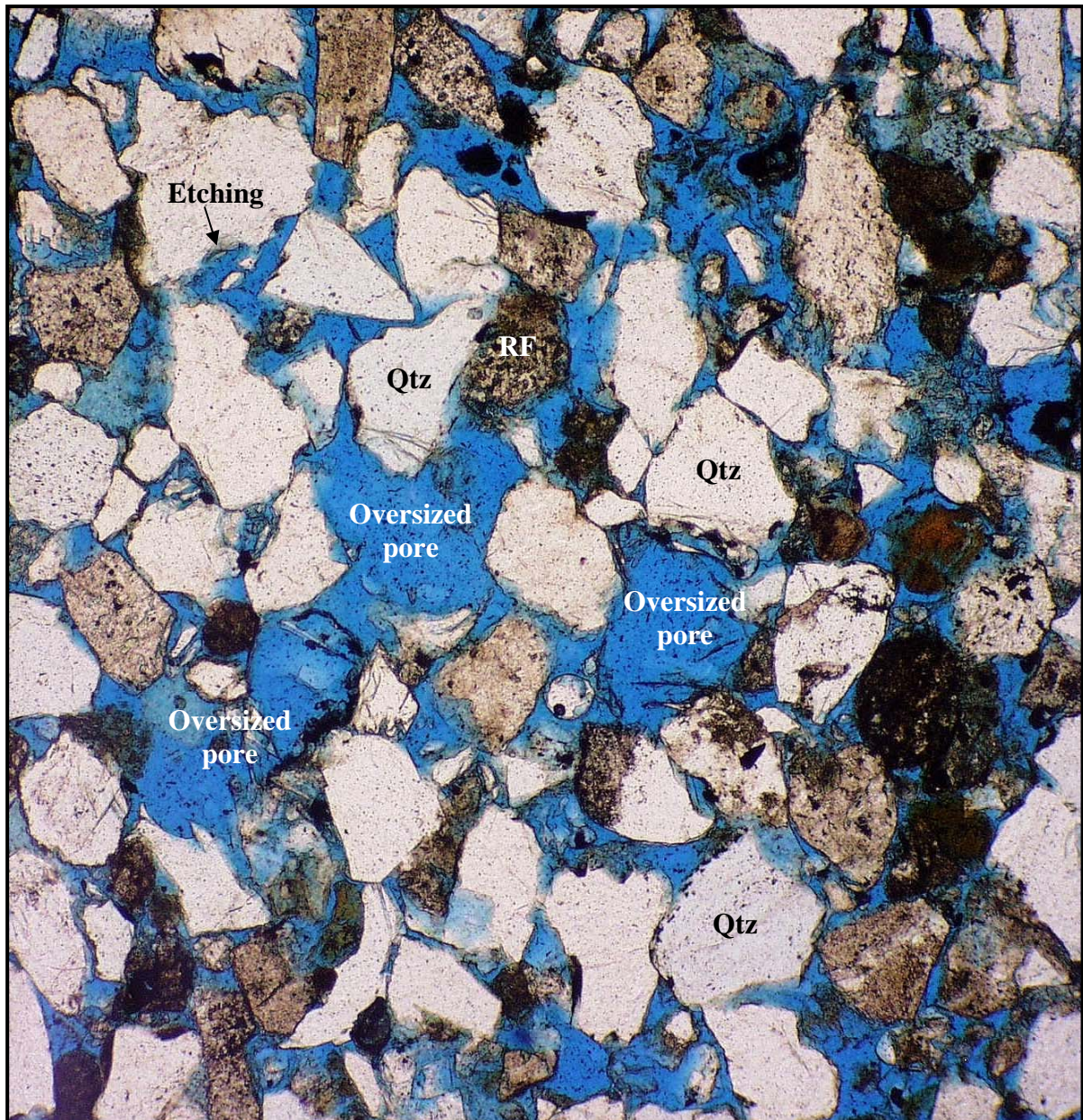


Figure 2.11

General field of view demonstrating the large amount of intergranular and dissolution porosity, 6% and 17% respectively from point count analysis. Grains are dominantly floating or have tangential contacts with minimal amounts of clay and matrix, therefore pore connectivity is high. Grain shapes are often irregular, confirming dissolution, probably an earlier carbonate phase.

Whelk-1, 1293.88m, plane light, 5 microns.

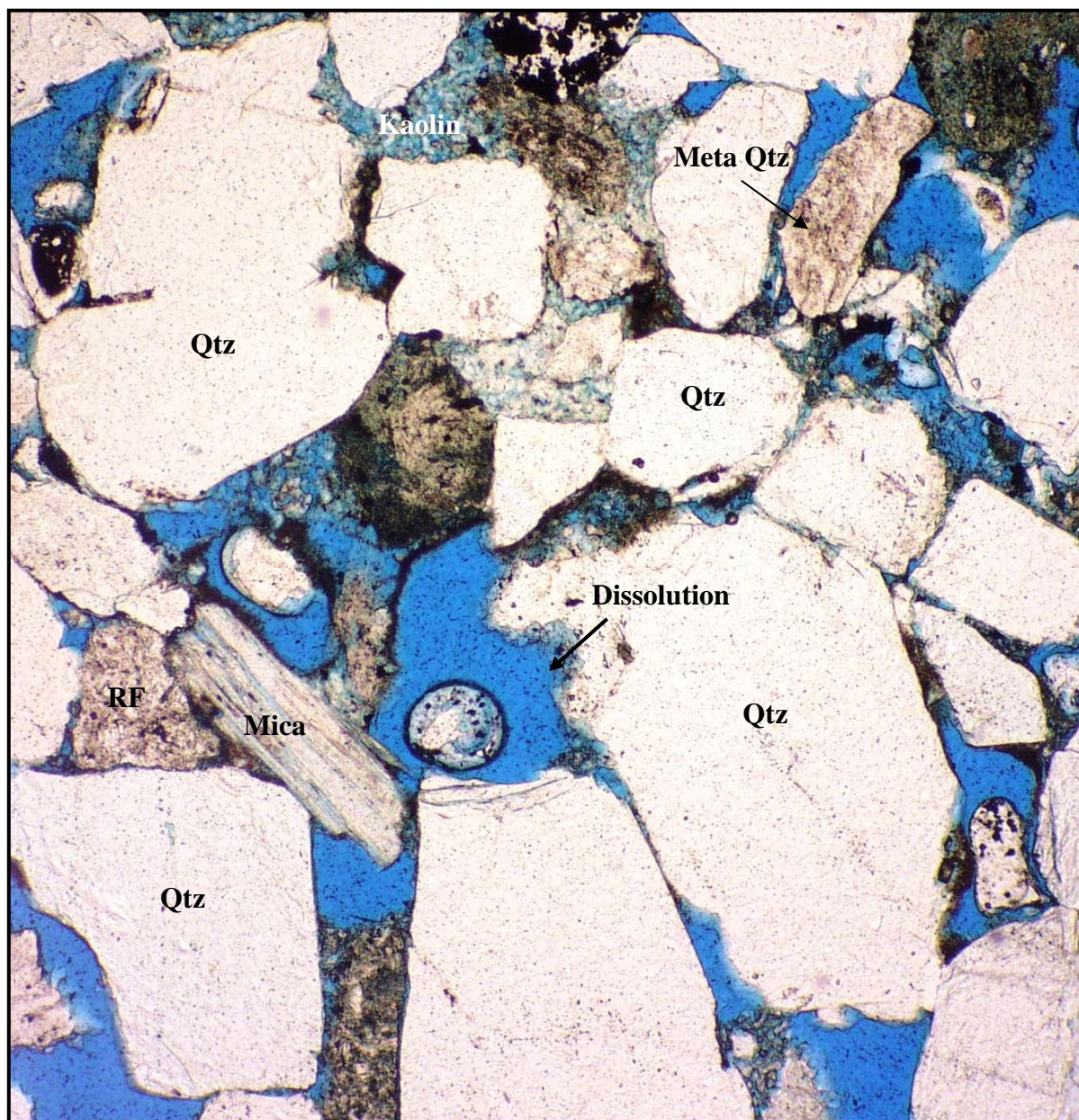


Figure 2.12

This sublitharenite, which has a bimodal grain size distribution, is dominantly comprised of quartz with some rock fragments, and intergranular, dissolution and micro-porosity (4%, 7.7% and 3.6% respectively). Sedimentary rock fragments include chert and siltstone, and metamorphic rock fragments comprise mica-bearing, quartz-rich sediment. Kaolin and carbonate contents are relatively low.

Prawn-A1, 2030.73m, plane light, 5 microns.

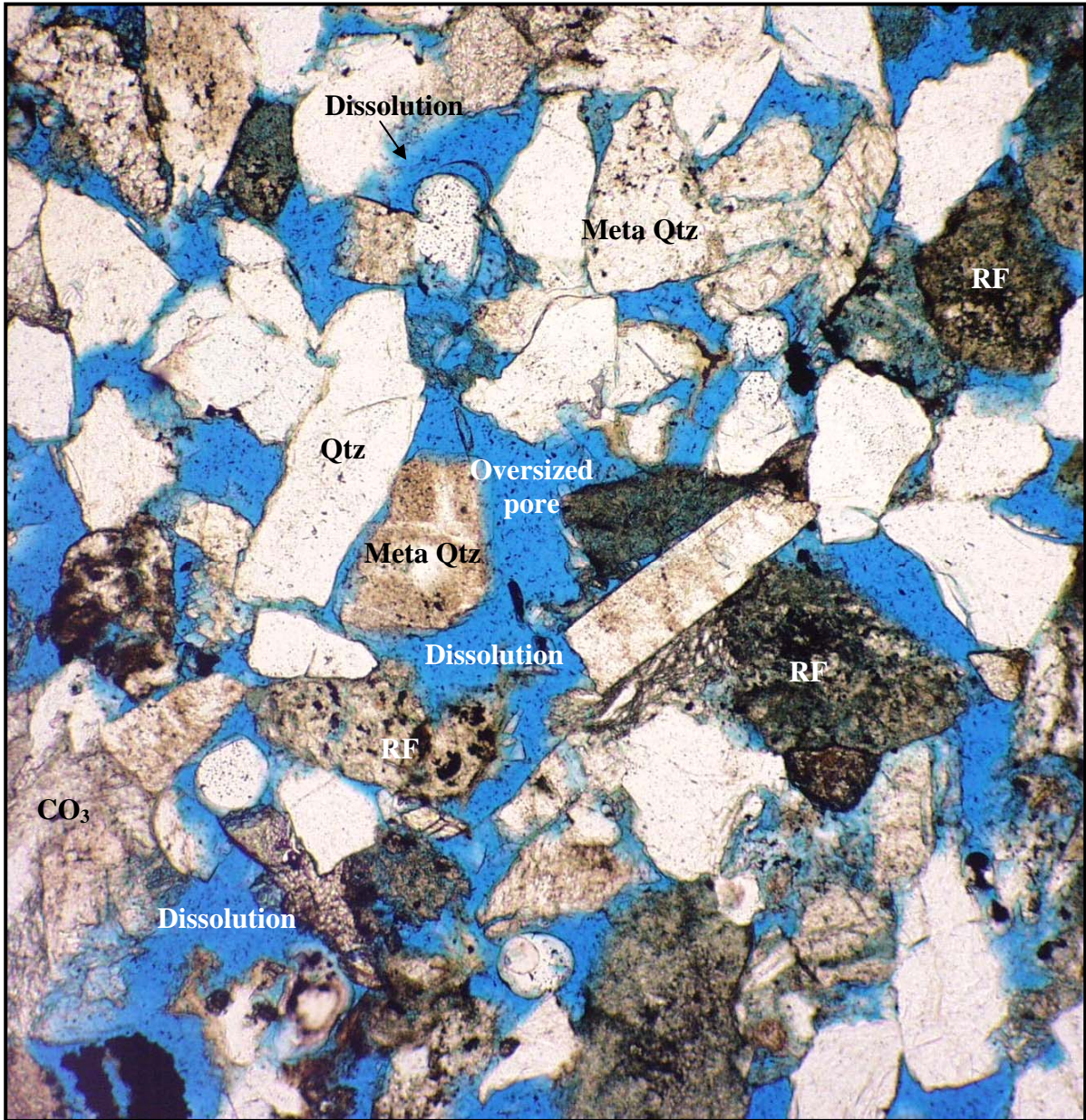


Figure 2.13

General field of view illustrating a porous sample comprised largely of quartz, rock fragments and secondary dissolution pores. The connectivity between pores is good, hence permeability is expected to be very good. Carbonate (siderite and dolomite) cement replaced grains and filled pore spaces. Secondary porosity by dissolution of a carbonate cement phase, suspected in other samples, is confirmed in the lower left quadrant of this field of view. Prawn-A1, 2032.25m, plane light, 5 microns

3. LITHOLOGY AND TEXTURE

Geographe-1 and Thylacine-2

Samples from the Thylacine Sandstone Member, Geographe-1 and Thylacine-2, are comprised of fine- to medium-grained, poor to moderately sorted sublitharenites (Figure 3). These sandstones are lithologically very similar to one another, excluding Geographe-1 1839.5m, 1909.8m and Thylacine-2 2229.62m which are largely dominated by authigenic carbonate. Laminae and planar bedding are outlined by changes in grain size and stringers of organic matter. Grain shape is typically angular to sub-rounded with low to moderate sphericity. Grain size ranges from clay to pebbles and commonly has a unimodal distribution.

Whelk-1 and Prawn-A1

Samples analysed from Whelk-1 and Prawn-A1 represent time equivalent sediments to the Thylacine Sandstone Member, however they differ slightly in composition to that of Geographe-1 and Thylacine-2, and probably indicate a more proximal environment. The sediment is composed of fine- to coarse-grained, poor to well sorted sublitharenites, interbedded with minor mudstones. Grains are typically angular to sub-rounded with low to high sphericity.

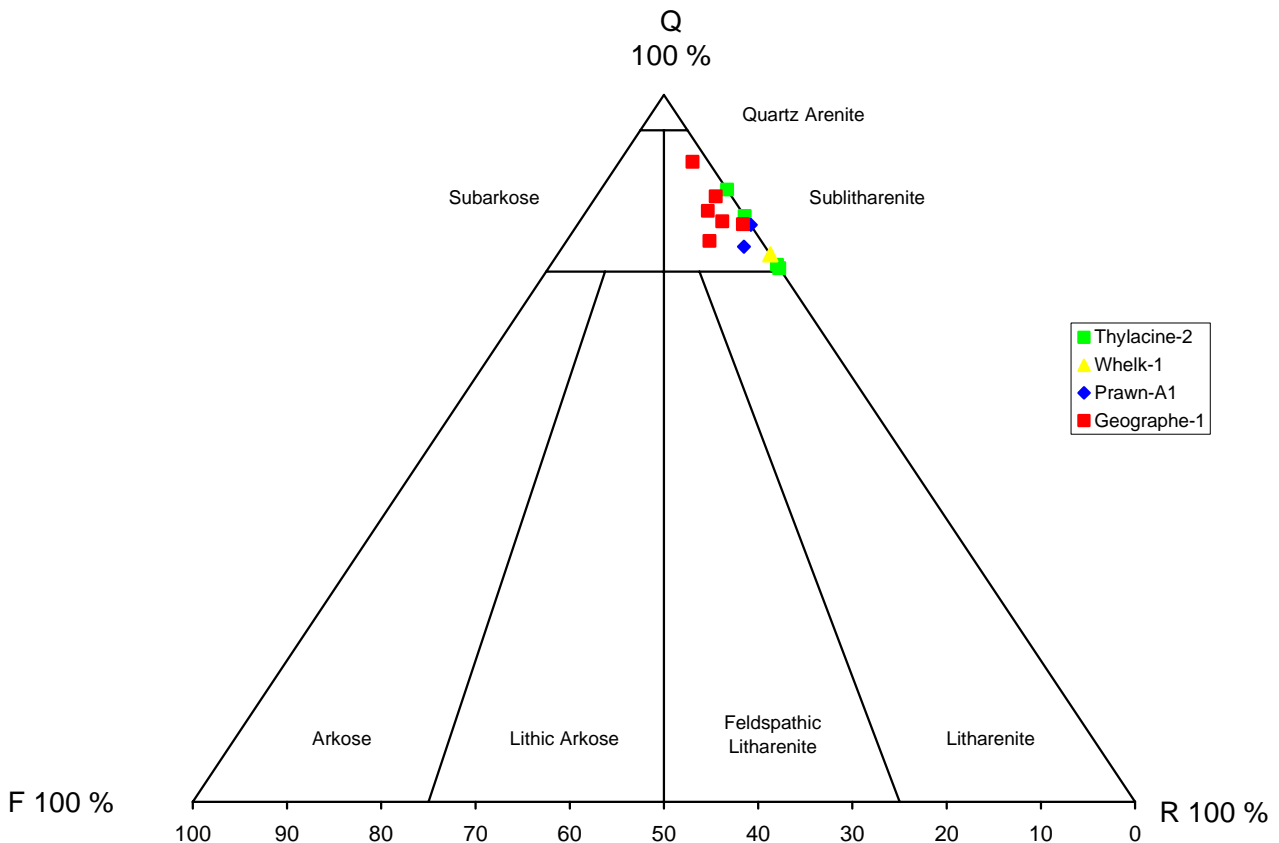


Figure 3: Folk classification for sandstones from Geographe-1, Thylacine-2, Whelk-1 and Prawn-A1. This plot is biased to the lithic portion of the triangle as many feldspars are dissolved, altered to kaolin or replaced by carbonate.

4. DETRITAL MINERALOGY

Geographe-1 and Thylacine-2

Detrital grains in the sublitharenites of Geographe-1 and Thylacine-2 are very similar in composition. Quartz and lithics are more abundant in the sandstones but all other grains (feldspars, micas and accessory minerals) are present in approximately equal amounts. Detrital quartz grains comprise between 34 and 40 percent of total rock composition. Monocrystalline (unstrained) quartz typically has straight and sutured crystal boundaries, characteristic of an igneous source. Polycrystalline (strained) quartz grains often constitute less than 13 percent. Twinned and zoned feldspars are rare and include both K-feldspar (microcline) and plagioclase. Sedimentary lithics comprise chert, mudstone and rare siltstone. Metamorphic lithics of shale, micaceous schist and quartzite are apparent. These lithics might reflect reworking of other sedimentary sequences and/or a metamorphic influence.

Whelk-1 and Prawn-A1

Samples within Whelk-1 and Prawn-A1 are compositionally very similar to one another, however differ slightly from Geographe-1 and Thylacine-2. Quartz with straight and sutured boundaries is the dominant detrital grain, constituting between 42 and 55 percent of the total rock volume. Sedimentary rock fragments are abundant in each of the samples, constituting largely of chert. Quartzite metamorphic and igneous rock fragments are also present in reasonable amounts (up to 5 percent total rock volume). K-feldspar and plagioclase are rare and are typically partially dissolved. Mica (2%) and accessory minerals also occur in trace to minimal amounts.

5. AUTHIGENIC MINERALOGY AND DIAGENETIC ALTERATION

Geographe-1 and Thylacine-2

Diagenetic alteration involved phases of mechanical compaction due to burial, dissolution, and precipitation of kaolin, carbonate, quartz and traces of chlorite and illite.

Kaolin is the most abundant clay recognized in the Thylacine Sandstone at Geographe-1 and Thylacine-2. Kaolin occurs as subhedral to euhedral, loosely packed stacks and elongate 'verms' partly filling primary and secondary dissolution pores and pore throats, and replacing grains. Loose kaolin is potentially subject to fines migration resulting in blocking of pore throats and reduction of permeability. Kaolin is characteristic of acidic pore waters, low to moderate temperature environments and appears to have formed from the alteration of feldspar and mica.

Sparry and micritic carbonate (siderite and calcite) are present in all the Thylacine Sandstone samples from Geographe-1 and Thylacine-2. Fe-rich spar formed slowly during the early phase of diagenesis. Quartz overgrowths formed prior to the pore filling carbonate spar and may have provided a rigid framework to reduce mechanical compaction. Micrite implies rapid rates of carbonate precipitation, which may have replaced spar, during late stage diagenesis.

The clear, poikilotopic twinned calcite spar that fills pores and replaces grains in the fine-grained sublitharenite (Geographe-1, 1909.8m) is thought to be late diagenetic burial cement, succeeding dissolution. Carbonate necessary for the precipitation of calcite was probably released from organic matter in the sediments during maturation and the source of Ca may have been provided by the corrosion of plagioclase feldspar.

Whelk-1 and Prawn-A1

There is minimal diagenetic alteration evident in the sandstone samples from Whelk-1 and Prawn-A1, most likely related to the shallower present day burial depth.

Kaolin is the dominant clay type observed, however in limited amounts (less than 4% of the total rock volume) compared with that observed at Geographe-1 and Thylacine-2. It is largely pore filling, often loosely packed and is therefore potentially subject to fines migration.

Authigenic quartz (SiO₂) is the dominant cement observed within the wells, ranging from approximately 4.7 to 8.7 percent. It occurs as syntaxial overgrowths on detrital quartz grains, frequently with euhedral and rhombohedral crystal terminations. The overgrowths form in optical continuity with the underlying quartz, and are visible in thin section due to the abundant inclusions or 'dust rims' at the boundary between detrital and authigenic quartz.

Carbonate, dominantly siderite and dolomite, occurs as a late spar typically replacing weaker grains. It is thought to succeed dissolution and often precipitates into secondary pores.

6. RESERVOIR QUALITY

Routine core analyses of Geographe-1, Thylacine-2, Whelk-1 and Prawn-A1 indicate porosity ranges from 1.32 to 32.31%. However, the visual estimates of porosity in thin section (two dimensions) when compared to core plug (three dimensions) data do not show a good correlation (Schulz-Rojahn & Phillips, 1989). Therefore, it is common for measured core porosity values to be higher. The most significant contribution from the thin section data is the type of pores present and their relative proportions.

There is very limited evidence that primary intergranular pores are preserved in Geographe-1 and Thylacine-2. Primary porosity is likely to have been occluded by a combination of compaction (plastic deformation of ductile grains, grain fracturing, pressure solution and grain rotation/slippage) and pore filling cements (carbonate, kaolin and quartz). In Whelk-1 and Prawn-A1 however, primary intergranular pores are preserved (? 6%) and there is only minor clay that would limit vertical permeability. The presence of intergranular pores may indicate that permeability is moderate.

At Geographe-1, Whelk-1 and Prawn-A1 porosity is dominated by secondary dissolution pores (ranging from 0 to 16.66%). Porosity created by dissolution of sedimentary minerals and authigenic cement is the most common porosity class. Dissolution of sedimentary material results from the selective dissolution of soluble grains, due to individual mineral stability. Secondary porosity is characterised primarily by the presence of oversized pores, dissolution remnants of minerals in pores and associated dissolution features (Schmidt and McDonald, 1979). Dissolution of feldspars and rock fragments creates the vast majority of the total volume of secondary sandstone porosity. The porosity is erratic in distribution and therefore associated permeability is low.

Thylacine-2 however is dominated by micropores associated with pore filling kaolin. Authigenic platelets, oriented perpendicular to the grain surface, would have spaces between the platelets. The associated porosity of micropores is high and expected permeability is low, due to the poor interconnectivity of the pores and size of the pore throats.

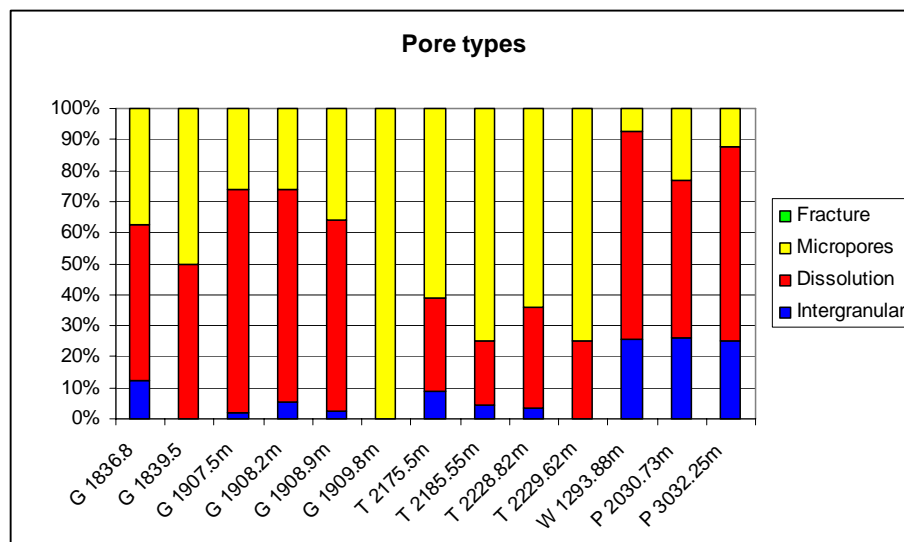


Figure 7: Pore types in the sandstones of Geographe-1 (G), Thylacine-2 (T), Prawn-A1 (P) and Whelk-1 (W) as identified from thin section